

Interleukin-12 Immunomodulation Delays the Onset of Lethal Peritoneal Disease of Ovarian Cancer

Courtney A. Cohen,¹ Amanda A. Shea,² C. Lynn Heffron,¹ Eva M. Schmelz,² and Paul C. Roberts¹

The omental fat band (OFB) is the predominant site for metastatic seeding of ovarian cancer. Previously, we highlighted the influx and accumulation of neutrophils and macrophages in the OFB following syngeneic ovarian cancer cell seeding as an important factor in the development of a protumorigenic cascade. Here we investigated localized immunomodulation as a means of promoting a successful protective response. As an important T_H1-type immunomodulator, interleukin (IL)-12 has previously been investigated clinically as an anticancer therapeutic. However, systemic IL-12 administration was associated with serious side effects, galvanizing the development of immune or accessory cells engineered to express secreted or membrane-bound IL-12 (mbIL-12). Using an mbIL-12-expressing cell variant, we demonstrate that localized IL-12 in the tumor microenvironment significantly delays disease development. The mbIL-12-mediated decrease in tumor burden was associated with a significant reduction in neutrophil and macrophage infiltration in the OFB, and correlated with a reduced expression of neutrophil and macrophage chemoattractants (CXCL1, -2, -3 and CCL2, -7). Vaccination with mitotically impaired tumor cells did not confer protection against subsequent tumor challenge, indicating that IL-12 did not impact the immunogenicity of the cancer cells. Our findings are in agreement with previous reports suggesting that IL-12 may hold promise when delivered in a targeted and sustained manner to the omental microenvironment. Furthermore, resident cells within the omental microenvironment may provide a reservoir that can be activated and mobilized to prevent metastatic seeding within the peritoneum and, therefore, may be targets for chemotherapeutics.

Introduction

OVARIAN CANCER HAS one of the highest incidence-to-death ratios due to its asymptomatic nature, the lack of early detection tools, and the high prevalence of metastases at the time of discovery (Allen and others 2012; Hunn and Rodriguez 2012). When ovarian cancer cells exfoliate from the primary tumor and are dispersed in the peritoneal cavity, initial metastatic outgrowths form within the omental fat band (OFB) (Gerber and others 2006; Krishnan and others 2012). The OFB is composed of adipose tissue interspersed with immune cell aggregates or “milky spots,” consisting of leukocytes, stem and progenitor cells, fibroblasts, and endothelial cells, collectively referred to as the stromal vascular fraction (SVF). Due to its important role in immune surveillance of the peritoneal cavity and its ability to mount innate and adaptive immune responses (Krist and others 1998; Rangel-Moreno and others 2009; Gray and others 2012), the OFB is considered a secondary lymphoid organ. Ovarian cancer cells readily adhere to “milky spots” and initiate a signaling cascade that promotes establishment of a protumorigenic microenvironment within the OFB (Sorensen and others 2009; Cohen and others 2013b). Thus, the OFB is typically removed as a preventative measure during tumor debulking, leaving women

more susceptible to subsequent peritoneal infections (Krist and others 1995; Gray and others 2012).

We have previously shown that the OFB is a unique immunoregulatory fat depot and that ovarian cancer cell seeding is associated with a protumorigenic signaling cascade supportive of rapid tumor outgrowth (Cohen and others 2013a, 2013b). Protumorigenic changes included an influx of tumor-associated macrophages (TAM) and tumor-associated neutrophils (TAN), and a significantly elevated expression of chemotactic signals for these cells. In contrast, parity was associated with a tumor-refractory phenotype that included inherent changes in the OFB transcriptome and cellular composition, leading to a significant reduction in TAM/TAN infiltration and disease severity (Cohen and others 2013b). Together, these findings highlight the importance of the OFB cellular composition in modulating the tumor microenvironment, and thus, the OFB may represent a target for antimetastatic immunotherapies.

IL-12 is a potent immunomodulatory cytokine that has been utilized in both laboratory and clinical settings as an anticancer therapeutic agent (see recent review Lasek and others, 2014). Tumor regression or suppression through soluble IL-12 immunotherapy has been documented in a wide variety of *in vivo* cancer models, including ovarian,

¹Department of Biomedical Sciences and Pathobiology, Virginia-Maryland College of Veterinary Medicine and ²Department of Human Nutrition, Foods, and Exercise, Virginia Polytechnic Institute and State University, Blacksburg, Virginia.

renal, gastrointestinal, and mammary carcinomas, melanomas, and lymphomas. The magnitude of outcome varies with tumor type, cytokine dose, and route of administration (Bajetta and others 1998; Rook and others 1999; Motzer and others 2001; Colombo and Trinchieri 2002; Ansell and others 2006; Del Vecchio and others 2007). IL-12 helps drive adaptive immune responses by polarizing naive CD4⁺ cells toward a T_H1 phenotype, inducing IFN- γ secretion by T and natural killer (NK) cells, stimulating differentiation of cytotoxic CD8⁺ cells, and increasing the activity of NK cells (Kalinski and others 1999; Yoo and others 2002; Curtsinger and others 2003; Trinchieri 2003). In the tumor microenvironment, IL-12 treatment can reactivate and sustain tumor-specific memory CD4⁺ T cells and polarize responses toward a protective T_H1 phenotype (Wesa and others 2007). In addition, it has potent antiangiogenic properties as a result of IFN- γ -induced upregulation of chemokines Cxcl9 and Cxcl10 (Nastala and others 1994). Thus, IL-12 promotes an antitumorigenic activity through multiple pathways.

Initial clinical trials utilizing systemic administration of IL-12 were largely unsuccessful due to severe side effects because of widespread IL-12 diffusion to the neighboring healthy tissues (Atkins and others 1997; Leonard and others 1997; Lenzi and others 2002; Lenzi and others 2007). Targeted IL-12 administration limits these undesirable effects and provides varying degrees of tumor regression or suppression, associated with increased CD8⁺ effector T- and NK-cell activity (Tahara and others 1994; Tahara and others 1995; Lim and others 2010; Pan and others 2012). In ovarian cancer, intraperitoneal (i.p.) injection of IL-12 alone or within a polymer delivery system promoted modest tumor regression in phase 1 clinical trials (Lenzi and others 2007; Anwer and others 2010). However, widespread dispersal throughout the peritoneal cavity induced dangerous side effects, highlighting the need for a more localized strategy.

In this study, we have assessed how the OFB-immune microenvironment responds to the challenge with tumor cells of varying metastatic efficacies to gain further insights into the signals that contribute to a successful protumorigenic niche. In parallel, we evaluated whether membrane-bound IL-12 (mbIL-12), when expressed directly on the tumor cell surface, could disrupt the protumorigenic signaling cascade and delay or inhibit tumor outgrowth within the peritoneal cavity. Our results demonstrate that localized expression of mbIL-12 can modulate the OFB microenvironment toward a tumor refractory state, delaying the onset of severe disease manifestations. This work highlights the targets that could be disrupted or modulated for improved therapeutic intervention against metastatic ovarian cancer. A more comprehensive understanding of the dynamic cellular interactions during metastatic outgrowth is critical for the development of treatment strategies to effectively target the tumor microenvironment at the time of disease discovery.

Methods and Procedures

Cell lines

The mouse ovarian surface epithelial (MOSE) cell model utilized in this study was derived from C57BL/6 mice and has been extensively characterized both *in vitro* and *in vivo* (Roberts and others 2005; Creekmore and others 2011). From this model, we utilized for the present studies (1) the

nonmalignant MOSE-E (early) cells that do not form tumors *in vivo*, (2) a firefly luciferase (FFL) expressing variant of MOSE-E, MOSE-E_{FFLV}, which facilitates whole-body bioluminescence imaging of tumor cells, (3) the malignant MOSE-L_{EGFPV}, an enhanced green fluorescent protein (EGFP)-expressing MOSE-L variant that results in a slow-developing disease within the peritoneal cavity, and (4) the highly aggressive FFL-expressing MOSE-L variant (MOSE-L_{FFLV}) (Cohen and others 2013b; Anderson and others 2014).

In addition, we utilized a MOSE-L_{FFLV} cell line that constitutively expresses a membrane-bound version of the murine IL-12 gene. Briefly, a murine single-chain IL-12 p35p40 gene was amplified from pORF-mIL-12 (p35p40) (InvivoGen, San Diego, CA) and fused in frame to the transmembrane encoding region of the influenza HA gene to ensure efficient and constitutive cell surface expression (Khan and others 2014). Stable transfectants of mbIL-12-expressing cells were established by passaging in the presence of G418 and further selected based on surface immunofluorescence staining of IL-12 using an Alexa Fluor⁴⁸⁸-conjugated antimouse IL-12p40 monoclonal antibody (eBioscience, San Diego, CA); the highest IL-12-expressing subclone was expanded and designated MOSE-L_{FFLV/IL-12V}.

Cells were routinely maintained in a high-glucose Dulbecco's modified Eagle's medium (Invitrogen, Grand Island, NY), supplemented with 4% fetal bovine serum (Hyclone, Logan, UT), and 100 mg/mL penicillin and streptomycin. Puromycin (4 μ g/mL) and/or G418 (1.4 mg/mL) supplementation was used to maintain FFL- and mbIL-12-expressing variants, respectively. Cell proliferation was evaluated through an MTT assay, as previously described (Humpf and others 1998) at the indicated time points.

Animals

Twelve-week-old female C57BL/6 mice (Harlan Laboratories, Indianapolis, IN) were housed, 5 per cage, in a controlled environment (12 h light/dark cycle at 21°C) with free access to water and food (18% protein rodent chow; Teklad Diets, Indianapolis, IN). This strain is syngeneic for our cell model. Animals were allowed to acclimate for 1 week before tumor cell implant. Preliminary dosage experiments determined the optimal cell number of each cell line required to develop macroscopically visible tumors within a 21-day postinjection period. Based on these results, all subsequent studies were performed using 1×10^4 MOSE-L_{FFLV} and MOSE-L_{FFLV/IL-12V} cells, and 1×10^6 MOSE-L_{EGFPV} and MOSE-E cells injected i.p. in 300 μ L sterile calcium- and magnesium-deficient phosphate-buffered saline (PBS^{-/-}).

To determine the efficacy of mbIL-12, mice ($n=6$) were injected i.p. with 2.5×10^6 MOSE-L_{FFLV} or MOSE-L_{FFLV/IL-12V} and sacrificed at day 15 postinjection to compare the relative tumor burdens. For vaccination and subsequent challenge experiments, cells were treated before implantation with 50 μ g/mL mitomycin C (MMC; MOSE-L_{FFLV/MMC}, MOSE-L_{FFLV/IL-12V/MMC}) for 45 min at 37°C to prevent *in vivo* proliferation. Here, the mice ($n=8$ each) received i.p. injections of either PBS^{-/-} (control) or 1×10^6 MOSE-L_{FFLV/IL-12V}, and MOSE-L_{FFLV/MMC} or MOSE-L_{FFLV/IL-12V/MMC} cells. Five weeks postimplantation, 3 mice per group were sacrificed to confirm mitotic inactivation of MMC-treated cells and lack of tumor burden. The remaining mice ($n=5$ per group) received a subsequent i.p. challenge with 1×10^4 MOSE-L_{FFLV}

cells. After 5 weeks, all mice were euthanized by CO₂ asphyxiation. All animal work was performed in accordance with the guidelines approved by the Virginia Tech Institutional Animal Care and Usage Committee.

IVIS imaging

Whole-animal bioluminescence imaging was used to monitor tumor progression of FFL-expressing cancer cell lines. Mice were imaged using the IVIS100 Imaging System (Xenogen, Alameda, CA) and Living Image acquisition and analysis software (Caliper Life Science, Hopkinton, MA). Briefly, mice were injected with ketamine/xylazine i.p. (100 mg/kg/10 mg/kg body weight), after which they were injected i.p. with 150 mg/kg D-luciferin and images were taken 5 min later; the exposure time was 1 min.

Peritoneal cancer index

To quantify relative tumor burden at the time of sacrifice, the peritoneal cancer index (PCI) was determined as described previously (Cohen and others 2013b). Relative PCI scores were further validated by quantitative real-time PCR (qRT-PCR) analysis of FFL and EGFP gene expression, employed as tumor cell reporter genes.

Tissue and peritoneal serous fluid harvest

The OFB was harvested from each mouse, weighed, rinsed with PBS^{-/-}, and processed either for flow cytometry, placed into RNeasy Lysis Buffer (Qiagen, Valencia, CA), and stored at -80°C until analyses, or imaged for MOSE-L_{EGFPv} outgrowth through fluorescence microscopy. Resident peritoneal cavity cells were collected through peritoneal lavage with 5 mL of 1 mM EDTA in PBS^{-/-}. The effluent was centrifuged, subjected to erythrocyte lysis (155 mM NH₄Cl, 10 mM KHCO₃, 0.1 mM EDTA), and further processed for flow cytometric analysis as described below. The SVF of individual OFBs was isolated from digested tissue as described previously (Cohen and others 2013a). After digestion at 37°C for 45 min, cells were passed through a 40-μm cell strainer, erythrocytes were lysed, and single-cell suspensions were obtained and counted.

Flow cytometric analysis

Single-cell suspensions derived from OFB and peritoneal serous fluid (PSF) were washed in a flow buffer (2% BSA in PBS^{-/-}) and treated with Fc Block (BD Biosciences, San Jose, CA) for 10 min at 4°C. Cells were then incubated with antibodies specific for mouse CD45, CD11b, CD11c, F4/80, Ly6C, CD4, CD44, CD62L, B220, CD19, NK1.1, Ly6G (eBioscience) CD3, and CD8 (BD Biosciences) for 20 min at 4°C (clone name/number and fluorochrome available upon request). Before analysis, cells were washed twice and resuspended in PBS^{-/-} with propidium iodide for dead cell exclusion. Flow cytometry was performed on a FACSAria (BD Biosciences) and data were analyzed using FlowJo (TreeStar, Ashland, OR) software. Gating analysis was performed as previously described (Cohen and others 2013a, 2013b).

Quantitative real-time PCR

Individual OFBs were homogenized in Qiazol (Qiagen) and RNA was purified using an RNeasy Lipid Tissue Kit

(Qiagen) according to the manufacturer's instructions. The RNA concentration was determined using a NanoDrop1000 spectrophotometer. RNA was subjected to the iScript cDNA synthesis system (Biorad, Hercules, CA) according to the manufacturer's protocol. qRT-PCR was performed with 12.5 ng cDNA per sample using gene-specific SYBR Green primers (primer sequences are available upon request) designed with Beacon Design software. SensiMix SYBR and Fluorescein mastermix (Bioline, Taunton, MA) was used in a 15 μL reaction volume. qRT-PCR was performed for 42 cycles at 95°C for 15 s, 60°C for 15 s, and 72°C for 15 s, preceded by a 10-min incubation at 95°C on the iQ5 (Biorad). Melt curves were performed to ensure fidelity of the PCR amplicon. The housekeeping gene was *L19* (Cohen and others 2013a) and the ddCt method (Schmittgen and Livak 2008) was used to determine fold differences.

Statistical analysis

Data are expressed as mean ± standard error of mean. Flow cytometry and qRT-PCR data were analyzed using a one-way analysis of variance coupled with a Tukey *Post hoc* test in SigmaPlot (Systat Software, San Jose, CA). Differences were considered statistically significant at $P < 0.05$.

Results

We have previously shown that peritoneal implantation of MOSE-L cells leads to metastatic outgrowth at the OFB and throughout the peritoneal cavity (Roberts and others 2005; Cohen and others 2013b). More recently, we described a parity-associated immune microenvironment that was refractory to tumor outgrowth and delayed the development of the protumorigenic cascade associated with peritoneal dissemination of highly aggressive ovarian cancer cells (Cohen and others 2013b). To gain further insights into how the immune cell composition is modulated during cancer cell seeding, we investigated the seeding dynamics of ovarian cancer cells and the subsequent impact on the immune cell composition within the omental and peritoneal microenvironments as a function of time, metastatic potential, and the presence of the immunomodulator, IL-12; the latter was expressed in a membrane-bound formulation directly on the tumor cells. We postulated that local immunomodulation through tumor-bound surface IL-12 may provide a means to delay or inhibit tumor outgrowth within the peritoneal cavity.

MOSE cells rapidly localize to the OFB independent of their metastatic potential

To gain insight into the protumorigenic modifications that ensue following cancer cell seeding of the OFB, we compared 3 syngeneic cell lines of varying metastatic potential: the nontumorigenic MOSE-E_{FFLV}, the slow disease-developing, EGFP-expressing MOSE-L_{EGFPv}, and the highly aggressive, FFL-expressing MOSE-L_{FFLV}. Irrespective of their tumorigenic potential, all MOSE cells rapidly localized and accumulated within the OFB of female C57BL/6 mice following i.p. injection. Peritoneal implantation of 1×10^6 MOSE-L_{EGFPv} cells led to their localization at the OFB as early as 6 h post-implantation (Fig. 1A, B) with established outgrowths readily evident at 24 h postseeding (Fig. 1C, D). This was comparable with the dynamics of MOSE-E_{FFLV} and MOSE-L_{FFLV} (data not

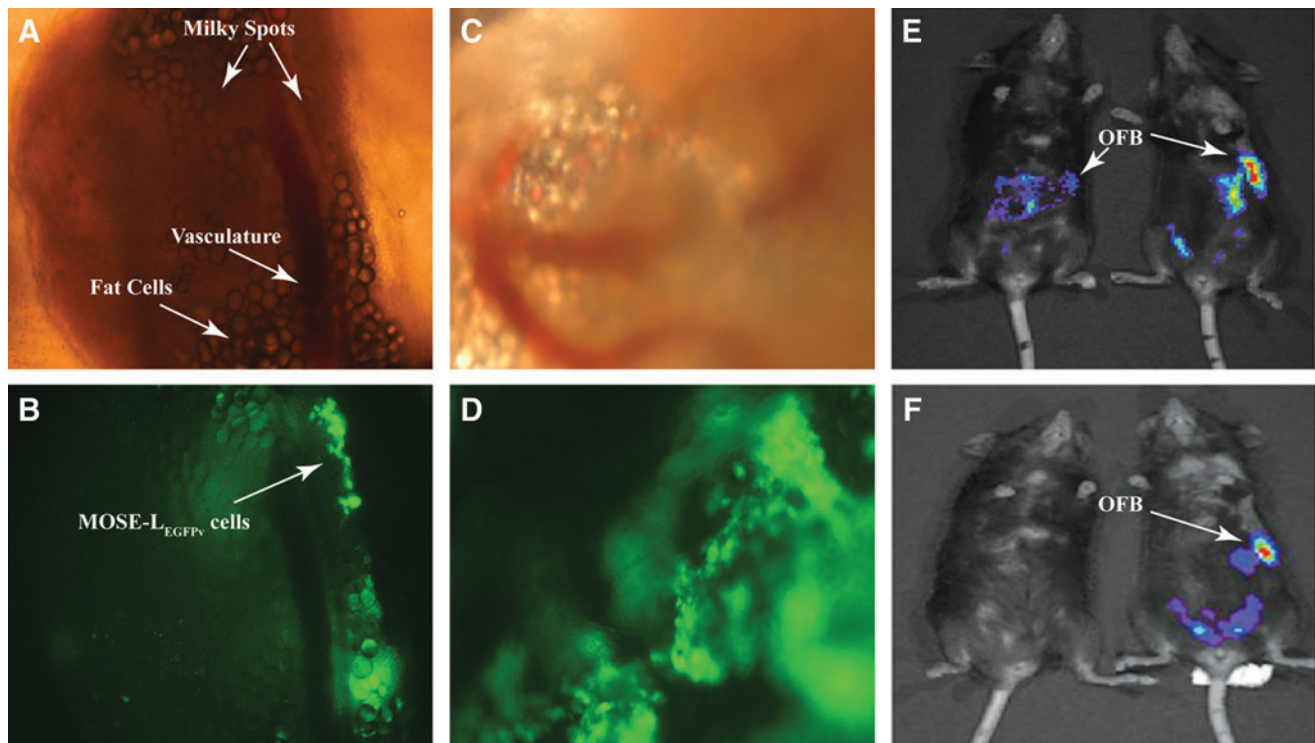


FIG. 1. Ovarian cancer cells localize to the omental fat band (OFB) within 6 h of intraperitoneal (i.p.) implantation. (A, B) The OFB at 6 h post-i.p. injection with 1×10^6 MOSE- L_{EGFP} cells. (C, D) The OFB at 24 h post-i.p. injection with MOSE- L_{EGFP} cells. (E) IVIS imaging of MOSE- E_{FFLV} and MOSE- L_{FFLV} i.p.-injected animals 24 h postinjection. (F) IVIS imaging of MOSE- E_{FFLV} and MOSE- L_{FFLV} i.p.-injected animals 8 days postinjection. Magnification: $40\times$ (A–D). EGFP, enhanced green fluorescent protein; FFL, firefly luciferase; MOSE, mouse ovarian surface epithelial.

shown), suggesting that an aggressive phenotype is not the determinant for the cells' rapid translocation to the OFB. Using whole-body bioluminescence imaging, we next monitored the peritoneal dissemination of MOSE- E_{FFLV} and MOSE- L_{FFLV} cells over time in live animals. While all FFL-expressing cell variants were readily detectable at 24 h postinjection (Fig. 1E), the signal was absent at day 8 in animals receiving MOSE- E_{FFLV} cells (Fig. 1F, left), suggesting either clearance by innate defense mechanisms or an inability to establish a protumorigenic microenvironment conducive for cell survival. In contrast, aggressive MOSE- L_{FFLV} cells remained detectable at day 8 and continued to disseminate throughout the peritoneal cavity until animals reached established endpoint criteria (Fig. 1E, F, right).

Expression of mbIL-12 on MOSE- L_{FFLV} does not alter in vitro growth rate or overall gene expression profile

Due to its potent T_H1 -polarizing activity and reported antitumorigenic effects, we investigated the potential of targeted IL-12 immunotherapy to manipulate the OFB microenvironment during cancer cell seeding and outgrowth. Specifically, we utilized mbIL-12, expressed directly on the surface of our aggressive cancer cell line (MOSE- $L_{FFLV/IL-12v}$). This allowed us to assess the impact of immunomodulation in a highly contained and localized manner, without the detrimental systemic release of IL-12 commonly associated with soluble formulations. Before *in vivo* studies, we confirmed that IL-12 was expressed at the cell surface of MOSE- $L_{FFLV/IL-12v}$ cells by live cell indirect immunofluorescence microscopy (Fig. 2A, B). Importantly, expression of mbIL-12 did not

alter the *in vitro* growth rate of MOSE- $L_{FFLV/IL-12v}$ compared with the parental line (Fig. 2C).

Using qRT-PCR analysis, we also evaluated the expression of a panel of cytokines and chemokines that can directly impact the establishment of a protumorigenic niche. The gene expression profiles of MOSE- $L_{FFLV/IL-12v}$ and its parental MOSE- L_{FFLV} were comparable, indicating that mbIL-12 incorporation did not alter expression of these genes (Fig. 2D). Of note, all MOSE lines, including the nonmalignant MOSE-E cells, expressed high levels of *Cxcl12*, a chemokine important for the recruitment of macrophages in a breast cancer animal model (Welford and others 2011). Cytokines involved in the recruitment and proliferation of monocytes (*Csf1*, *Ccl2*, *Ccl7*) were also highly expressed in all cell lines. The nonmalignant MOSE-E cell line exhibited a significantly lower expression of neutrophil chemoattractants *Cxcl1* and *Cxcl5* compared with its malignant counterparts ($P < 0.001$). This is noteworthy because a reduction in the expression of these chemoattractants has been associated with delayed disease progression and outgrowth in the OFB (Cohen and others 2013b). As expected, expression of the reporter genes EGFP, FFL, and IL-12 was only detected in their respective cell lines.

mbIL-12 reduces peritoneal tumor burden and extends survival

To evaluate the protective effect of mbIL-12 *in vivo*, peritoneal tumor burden was measured following i.p. implantation of 2.5×10^6 MOSE- $L_{FFLV/IL-12v}$ or MOSE- L_{FFLV}

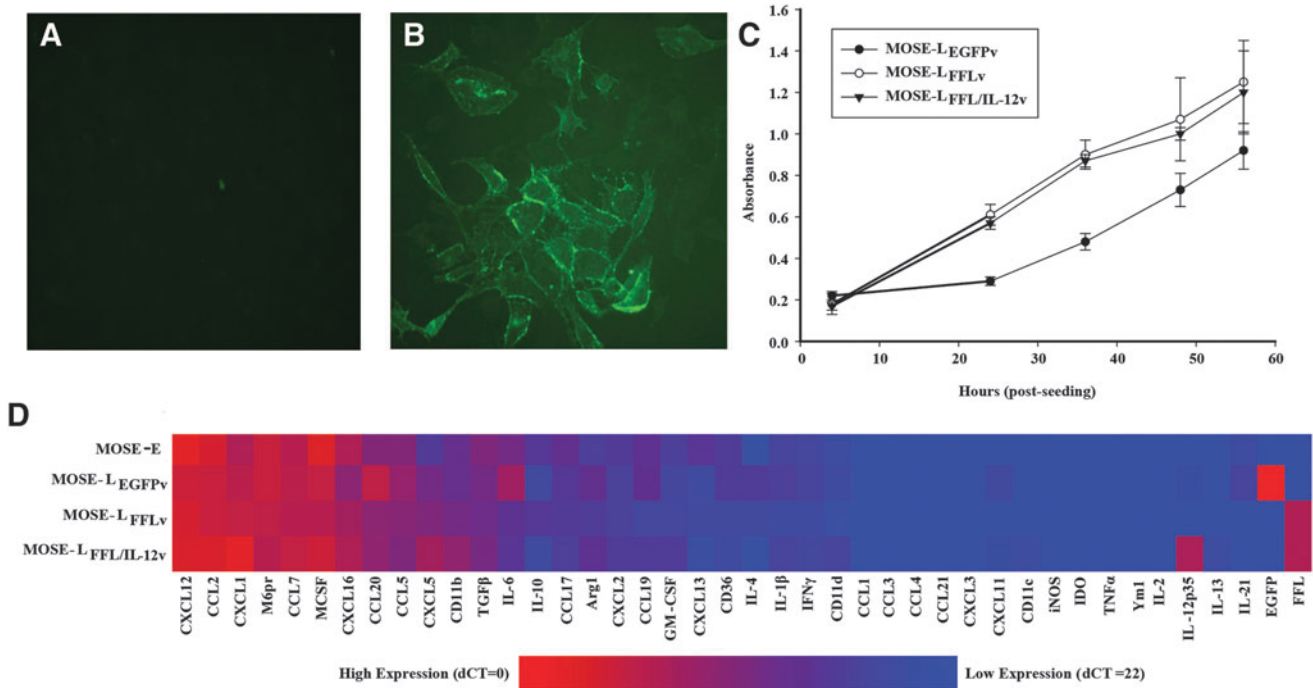


FIG. 2. MOSE cell line phenotypic characterization. Live cell surface IL-12 staining of (A) MOSE-L_{FFL} and (B) MOSE-L_{FFL/IL-12v} (Magnification: 200 \times) (C) *in vitro* proliferation, MTT assay. (D) Gene expression of MOSE cell line variants. IL, interleukin.

cells. This dose of MOSE-L_{FFL} cells was highly lethal, with C57BL/6 mice reaching established endpoints within 15 days (data not shown). This corresponded to a high tumor burden determined postmortem (Fig. 3A, $P < 0.01$). In contrast, animals that received the same dose of MOSE-L_{FFL/IL-12v} cells exhibited a significantly decreased tumor burden.

To encourage protective immunoregulatory events that may have been masked due to rapid tumor dissemination, in subsequent studies, animals were implanted with either a moderate (1×10^6) or low (1×10^4) dose of tumor cells. As shown in Fig. 3B, animals implanted with 1×10^6 MOSE-L_{FFL/IL-12v} cells had a significantly longer life span compared with animals receiving a low or moderate dose of MOSE-L_{FFL} (Fig. 3B, $P < 0.01$). At 3 weeks postimplantation, the tumor burden of mice injected with 1×10^4 MOSE-L_{FFL/IL-12v}

was significantly lower than in those animals receiving MOSE-L_{FFL}, but similar to that of mice injected with MOSE-L_{EGFPv} cells at a 100-fold higher dose (Fig. 3C, $P < 0.01$); however, peritoneal disease was not completely abrogated. Thus, surface expression of IL-12 reduced the outgrowth of aggressive cancer cells in the OFB and other organs in the peritoneal cavity, significantly extending the life span of these mice.

mbIL-12 delays polarization of the protumorigenic niche within the OFB and peritoneal cavity

To gain insight into the mechanisms behind the IL-12-mediated delay in disease development, we comparatively assessed the immune cell composition of the OFB and PSF as a consequence of MOSE-L_{FFL}, MOSE-L_{FFL/IL-12v},

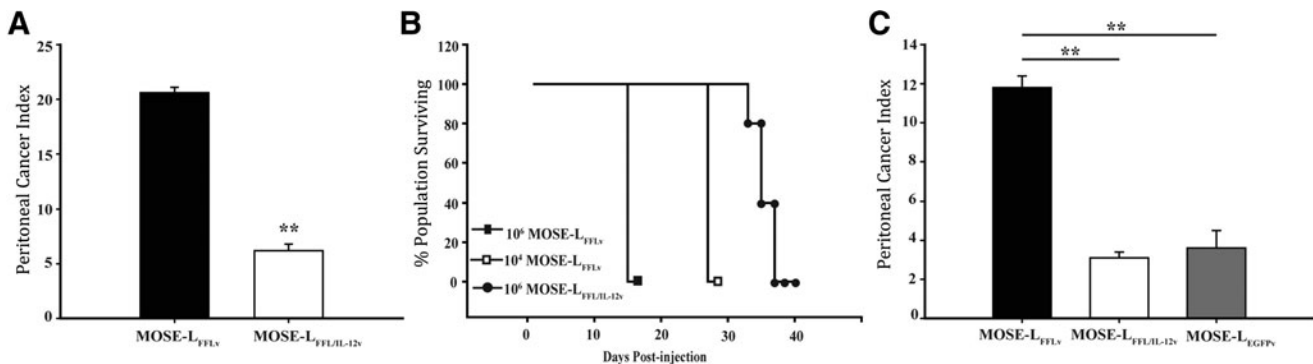


FIG. 3. Membrane-bound IL-12 (mbIL-12) reduces ovarian cancer cell tumorigenicity. (A) Peritoneal cancer index (PCI) 15 days postinjection of 2.5×10^6 cells i.p. ($n = 6$) (B) Survival curve 10^6 MOSE-L_{FFL}, 10^4 MOSE-L_{FFL}, and 10^6 MOSE-L_{FFL/IL-12} cells. (C) PCI 3 weeks postinjection i.p. of 1.0×10^4 MOSE-L_{FFL}, 1×10^4 MOSE-L_{FFL/IL-12v}, or 1×10^6 MOSE-L_{EGFP} cells ($n = 15$). ** $P < 0.01$.

MOSE- L_{EGFPv} , or mock i.p. injection (PBS $^{-/-}$) through flow cytometry analysis. Macroscopically, the OFBs of MOSE- L_{FFLV} mice were overwhelmed by tumor tissue 21 days postimplantation, with no detectable adipose tissue remaining. In contrast, the OFB of MOSE- $L_{FFL/IL-12v}$ and MOSE- L_{EGFPv} animals retained adiposity, although tumor nodules were evident. As noted above, the overall tumor burden throughout the peritoneal cavity was also significantly reduced in the latter 2 groups compared with MOSE- L_{FFLV} (Fig. 3C).

Flow cytometry analysis of the OFB revealed cell line-associated differences in leukocyte populations. MOSE- L_{FFLV} outgrowth in the OFB resulted in a significant decrease in the proportion of lymphocytes and a concomitant increase in monocyte/granulocytes, compared with PBS-injected control animals (Fig. 4A, $P < 0.01$). Neither the animals that received MOSE- $L_{FFL/IL-12v}$ nor those that received MOSE- L_{EGFPv} exhibited this shift. In MOSE- L_{FFLV} mice, there was a significantly low percentage of CD3 $^{+}$, CD19 $^{+}$, and NK1.1 $^{+}$ cells, while concomitantly more F4/80 $^{+}$ cells were detected (Fig. 4B–E, $P < 0.01$). In contrast, implantation of mbIL-12-expressing cells resulted in an immune microenvironment profile similar to that seen with our slow-developing disease model, MOSE- L_{EGFPv} , highlighted by significant increases in CD3 $^{+}$ T-cell numbers compared with PBS-injected animals (Fig. 4B, $P < 0.01$). Of note, the proportion of CD19 $^{+}$ B cells decreased as a result of MOSE- L_{EGFPv} (but not MOSE- $L_{FFL/IL-12v}$) implants, although not to the extent of MOSE- L_{FFLV} levels.

F4/80 $^{+}$ macrophages in the OFB remained unchanged following both MOSE- $L_{FFL/IL-12v}$ and MOSE- L_{EGFPv} injections (Fig. 4C, D). Interestingly, the proportion of NK

1.1 $^{+}$ cells decreased in the OFB of MOSE- L_{EGFPv} animals ($P < 0.01$), but not in MOSE- $L_{FFL/IL-12v}$ animals (Fig. 4E). This could be due to direct interactions between localized mbIL-12 and NK1.1 $^{+}$ cells. In agreement with our previous report (Cohen and others 2013b), MOSE- L_{FFLV} implantation and outgrowth resulted in a significant accumulation of CD11b $^{+}$ Ly6G $^{+}$ Ly6C $^{+}$ TANs in the OFB (Fig. 4F, $P < 0.01$). Whereas TANs significantly accumulated in the OFB of the MOSE- L_{EGFPv} group, although not to the extent of MOSE- L_{FFLV} animals, they were virtually absent from the MOSE- $L_{FFL/IL-12v}$ OFB, mirroring levels observed in control mice (Fig. 4F). This suggests that localized mbIL-12 expression may negatively modulate the influx of TANs to the OFB, which could, in turn, delay the establishment of an aggressive protumorigenic microenvironment.

Given the importance of the PSF in ovarian cancer dissemination and metastasis, we evaluated it separately as an immunologically relevant microenvironment. The shift in lymphocytes:mono/granulocytes was even more marked in the PSF, where MOSE- L_{FFLV} implantation led to a 39.4% decrease in the former (Fig. 5A, $P < 0.01$). This loss of lymphocytes was largely reflected in the CD19 $^{+}$ population, with no significant difference in the levels of CD3 $^{+}$ cells noted (Fig. 5B, C). In addition, there was a significant increase in F4/80 $^{+}$ macrophages (Fig. 5D, $P < 0.01$) in MOSE- L_{FFLV} animals. Further characterization (FSC/SSC and differential CD11b/F480 surface staining) of these macrophages confirmed that they were largely confined to the small, infiltrating macrophage subset that is frequently elevated under inflammatory conditions (Ghoshn and others 2010). The proportion of the large resident peritoneal

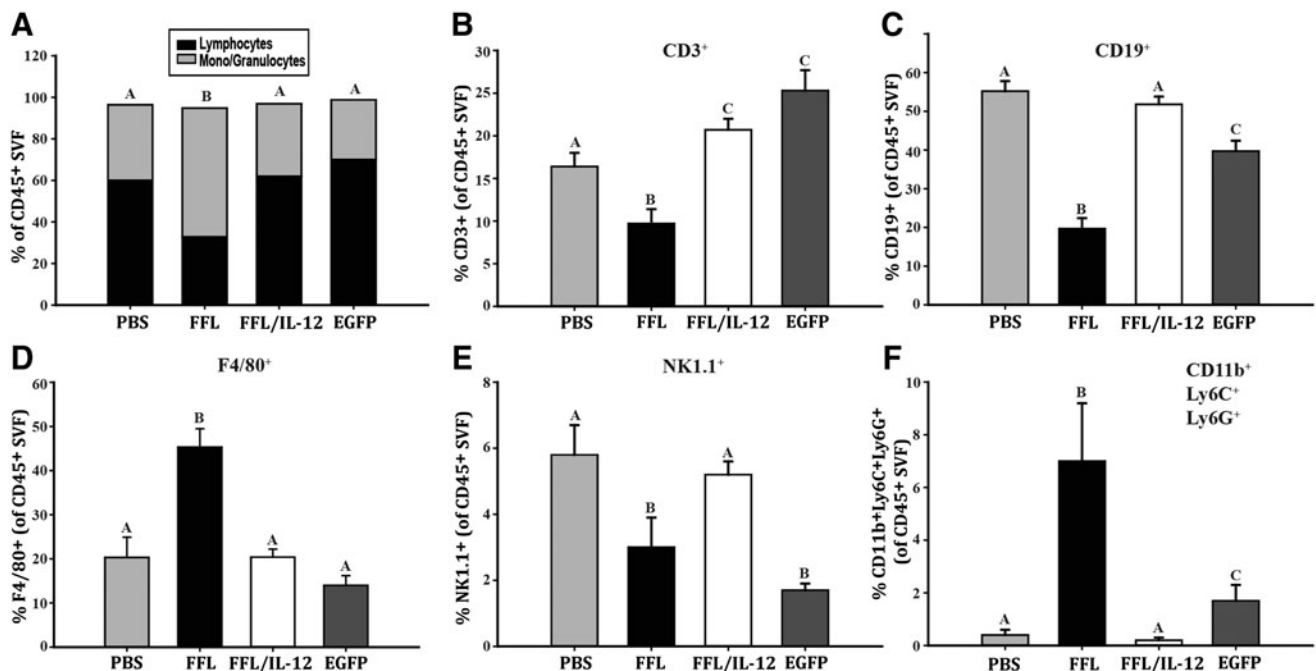


FIG. 4. mbIL-12 reduces ovarian cancer outgrowth-associated influx of macrophages and neutrophils to the OFB. (A) Proportion of lymphocytes to monocytes/granulocytes in the total CD45 $^{+}$ leukocyte fraction. (B) Proportion of CD3 $^{+}$ T cells in total leukocytes. (C) Proportion of CD19 $^{+}$ B cells in total leukocytes. (D) Proportion of F480 $^{+}$ macrophages in total leukocytes. (E) Proportion of NK1.1 $^{+}$ NK cells in total leukocytes. (F) Proportion of CD11b $^{+}$ Ly6C $^{+}$ Ly6G $^{+}$ tumor-associated neutrophils (TANs) in total leukocytes. Unlike letters (A–C) indicate significant differences between groups, $P < 0.05$. NK, natural killer.

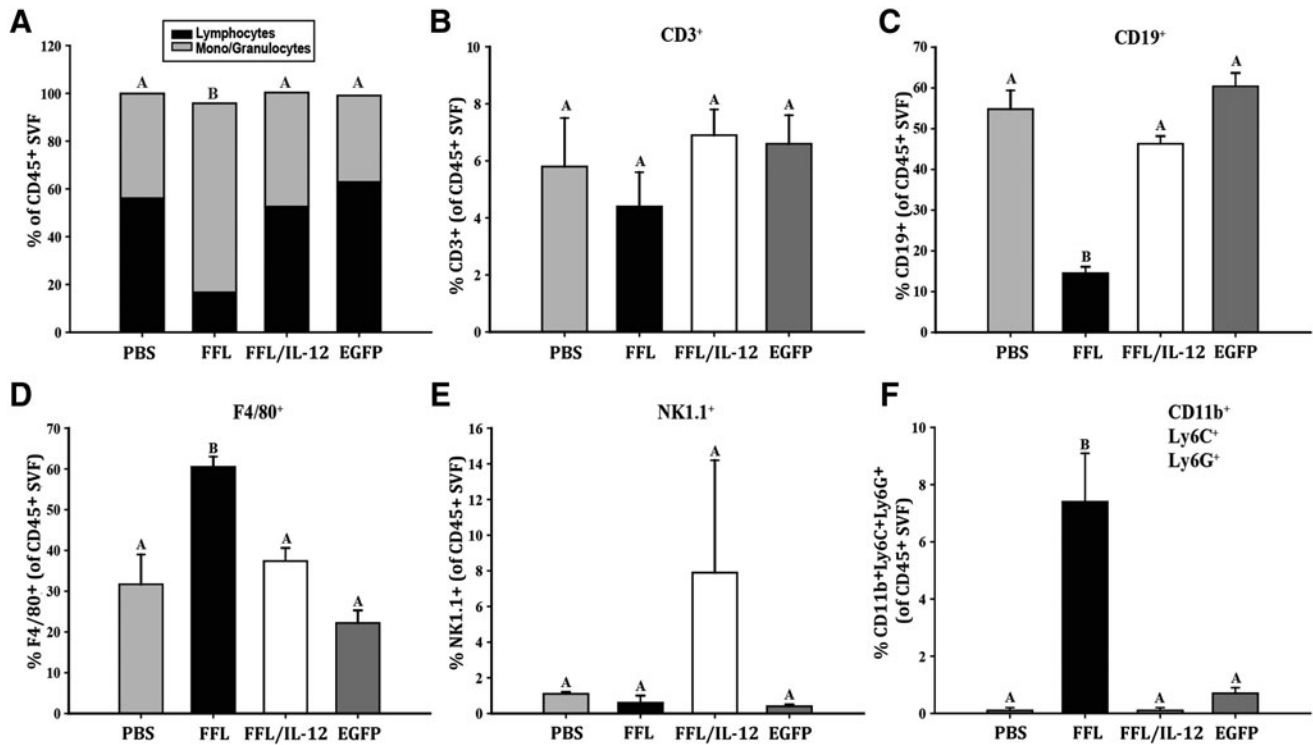


FIG. 5. mbIL-12 reduces ovarian cancer outgrowth-associated influx of macrophages and neutrophils to the peritoneal serous fluid. (A) Proportion of lymphocytes to monocytes/granulocytes in the total CD45⁺ leukocyte fraction. (B) Proportion of CD3⁺ T cells in total leukocytes. (C) Proportion of CD19⁺ B cells in total leukocytes. (D) Proportion of F480⁺ macrophages in total leukocytes. (E) Proportion of NK1.1⁺ NK cells in total leukocytes. (F) Proportion of CD11b⁺Ly6G⁺Ly6C⁺ TANs in total leukocytes. Unlike letters (A–C) indicate significant differences between groups, $P < 0.05$.

macrophage subset, the most abundant peritoneal macrophage subset in the homeostatic state, remained relatively constant (data not shown).

There were no statistically significant changes in the NK1.1⁺ populations in the PSF as a result of MOSE cell seeding, although one mouse in the MOSE- $L_{FFL/IL-12v}$ group presented with a large NK1.1⁺ population that was considered an outlier (Fig. 5E). Similar to the OFB, TAN levels were significantly increased in the PSF following MOSE- L_{FFLV} peritoneal implantation (Fig. 5F, $P < 0.01$). Together, these data suggest that the surface expression of IL-12 on highly aggressive MOSE- $L_{FFLV/IL-12v}$ cells within the peritoneal cavity serves to delay the recruitment of monocytes and TANs to the site of metastatic outgrowth.

Gene expression profiling supported the observed cancer-associated changes in the leukocyte composition in the OFB (Fig. 6). Compared with PBS-injected controls, the OFBs of MOSE- L_{FFLV} animals displayed significantly lower expression levels of *Ii2*, *Cxcl13*, and *Iil2* (Fig. 6A, $P < 0.01$), cytokines important for T-cell proliferation, B-cell chemoattraction, and T- and NK-cell activation, respectively. The latter was particularly interesting given the mitigating effect that mbIL-12 has on tumorigenicity. Several signals involved in inflammatory recruitment and proliferation (*Ccl5*, *Cd36*, *Gmcsf*, *Tnfx*) were also significantly reduced ($P < 0.01$) in MOSE- L_{FFLV} , compared with PBS control animals. The expression of neutrophil chemoattractants (*Cxcl1*, -2 , -5) was significantly upregulated in the OFB of MOSE- L_{FFLV} mice compared with controls, as were monocyte-associated *Arg1* and *Nos2* (Fig. 6B, $P < 0.01$). Most

notably, gene expression of all of these chemoattractants remained at PBS control levels in MOSE- $L_{FFLV/IL-12v}$ animals. Together, these data support the role of mbIL-12 in modulating the balance between a protective and a protumorigenic metastatic microenvironment. Moreover, none of the microenvironment-associated gene expression changes noted above was detected in the OFB of MOSE- L_{EGFPv} mice, further supporting their importance in aggressive disease development.

FFL cells expressing mbIL-12 retain their low immunogenicity and do not protect against tumor rechallenge

Given the convincing evidence of IL-12 efficacy as an antitumor therapeutic, as well as its vaccine-enhancing capacities (Khan and others 2014), we tested whether vaccination with mitotically inactive, mbIL-12-expressing MOSE- $L_{FFLV/IL-12v}$ cells would elicit an immune response that conferred protection against subsequent tumor challenge. To address this question, immunocompetent C57BL/6 female mice were injected i.p. with 1×10^6 MMC-treated MOSE- L_{FFLV} or MOSE- $L_{FFLV/IL-12v}$ cells or PBS (controls). After 5 weeks, the lack of tumor formation was confirmed and the remaining mice were challenged with 1×10^4 MOSE- L_{FFLV} cells (Fig. 7). Prior exposure to mitotically inactive malignant cells irrespective of the presence of mbIL-12 failed to elicit protective responses against a subsequent challenge with malignant cells. This suggests that surface expression of IL-12 either does not impact the poor

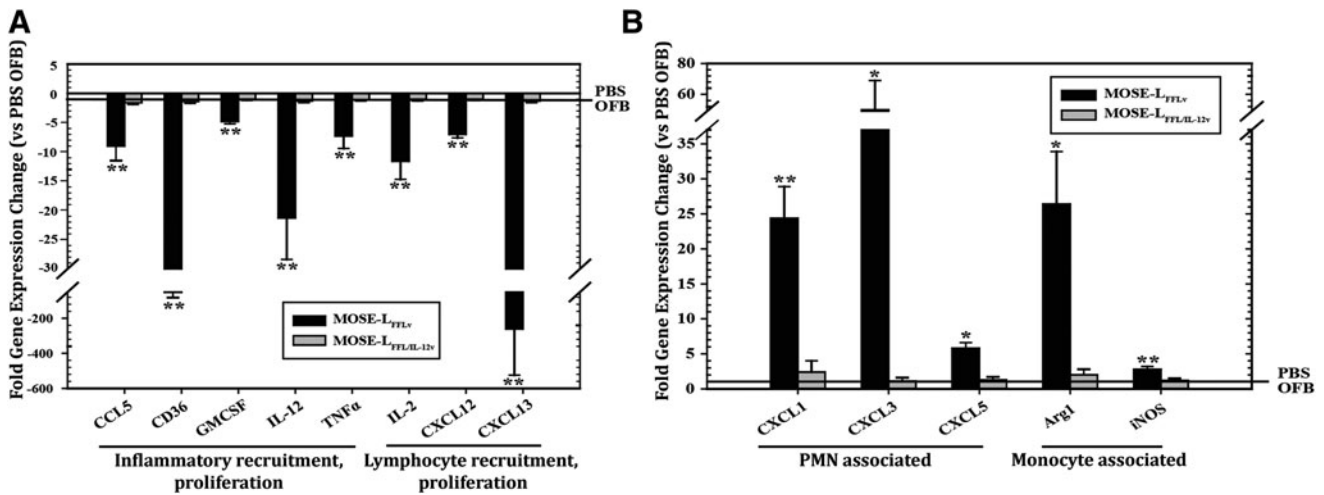


FIG. 6. Gene expression changes in the OFBs of MOSE-L_{F_{FLV}}- and MOSE-L_{F_{FLV}/IL-12_v}-bearing mice compared with mock-injected (PBS^{-/-}) mice. All genes displayed were significantly lower (A) or higher (B) than controls, **P* < 0.05, ***P* < 0.01. PBS, phosphate-buffered saline.

immunogenicity of our highly aggressive MOSE-L_{F_{FLV}} cell line or the rapid tumor growth was able to overwhelm the elicited immune response. Studies determining the changes in the elicited responses as a function of time and cancer cell presence are planned to evaluate these possibilities.

Discussion

Our recent studies have highlighted the importance of the immune modulation of omental and peritoneal microenvi-

ronments to generate refractory or permissive niches for disseminated ovarian cancer cells. The reduced neutrophil and macrophage infiltration of parous mice in the OFB changes its secretory profile and exerts tumor refractory properties (Cohen and others 2013b). In this study, we explored an immunomodulatory strategy to generate a non-permissive microenvironment that disrupts or delays the onset of peritoneal disease. To this end, we investigated the impact of mbIL-12 on the immune microenvironment of the OFB, a secondary lymphoid organ that acts as a reservoir for peritoneal leukocytes. It is the primary site of ovarian cancer metastasis and is seeded with cancer cells, irrespective of their aggressive potential within 6 h of implantation. The presentation of mbIL-12 on the surface of highly aggressive, ovarian cancer cells (MOSE-L_{F_{FLV}/IL-12_v}) resulted in a significant reduction in peritoneal tumor burden.

The significant reduction in lymphocyte populations (CD3⁺, NK1.1⁺, and CD19⁺), the concomitant increase in monocyte/granulocyte populations (TAMs and TANs), and a complete loss of adiposity in the OFB observed in mice implanted with MOSE-L_{F_{FLV}} was not observed in mice receiving MOSE-L_{F_{FLV}/IL-12_v} cells. The reduction in disease severity was associated with significantly decreased TANs in the OFB and PSF as well as a reduction in the gene expression levels of key TAN chemoattractants in the OFB. The significantly different leukocyte populations in the OFB, following implantation with aggressive versus slow-developing disease models, may represent responses that are primarily protumorigenic in contrast to those that maintain a balance between immunosuppression and tumor inhibition.

Of note, the IL-12-mediated protection was only transient. Although mbIL-12 mice lived significantly longer than those injected with the parental MOSE-L_{F_{FLV}}, the animals eventually succumbed to disease, suggesting that mbIL-12 may act by delaying the development of the protumorigenic cascade within the OFB and dampening the capacity to attract protumorigenic accessory cells. Given the extremely low 5-year survival rate in ovarian cancer patients, as well as the high rate of chemoresistant, recurrent disease, this extension in life span is significant and provides

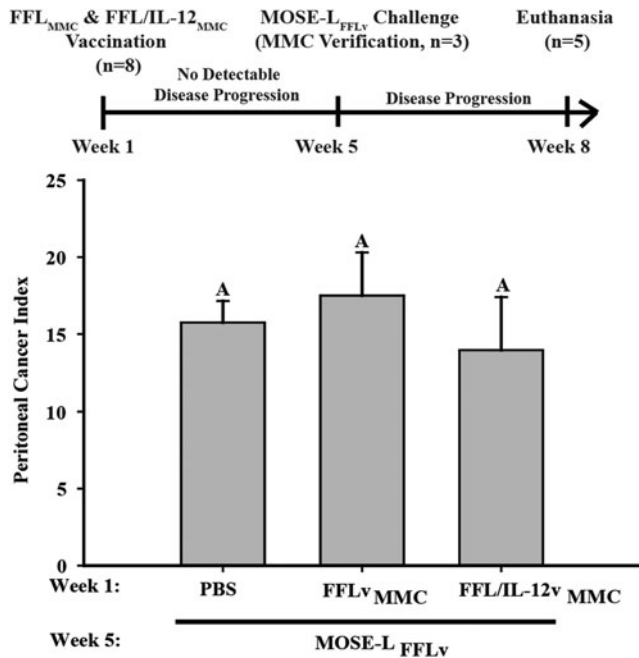


FIG. 7. mbIL-12 does not provide protection against subsequent challenge. PCI in mice (*n* = 5) treated with PBS^{-/-}, FFL_vMMC, or FFL/IL-12_vMMC at 1 × 10⁶ and challenged with 1 × 10⁴ MOSE-L_{F_{FLV}} at week 5. MMC, mitomycin-C; PCI, peritoneal cancer index.

valuable insight into the potential of immunomodulatory therapeutics to suppress peritoneal outgrowths.

IL-12 has been utilized in a wide variety of cancer models as a potent antitumorigenic therapeutic, although clinical applications have been hindered due to severe toxicity associated with systemic IL-12. Membrane-bound cytokines have been reported to enhance tumor immunogenicity over that of secreted cytokines, ultimately stimulating robust antitumor immune responses (Ling and others 1995; Jana and others 2003; Zhang and others 2011). Membrane-bound formulations are expected to act locally through cell–cell interactions, thereby reducing aberrant systemic signaling events. CT26 colon carcinoma cells, expressing either soluble or mbIL-12, displayed reduced metastatic potential, with the mbIL-12 CT26 variant eliciting potent, long-term protective immune responses (Pan and others 2012). Expression of mbIL-12 in subcutaneous fibrosarcoma cells was associated with induction of tumor-specific cytotoxic T lymphocyte responses and delayed tumor formation, but these were not fully protective against subsequent tumor challenge (Lim and others 2010). Our results are more in line with the latter study, in that long-term persistence of antitumor immune responses was not observed. Preconditioning the peritoneal microenvironment with mitotically inactive MOSE cells was not protective irrespective of mbIL-12 expression, confirming that MOSE cells are poorly immunogenic. Alternatively, if adaptive responses were elicited, they were insufficient to protect against the protumorigenic microenvironment that is rapidly established by the highly aggressive MOSE-L_{F_{FLV}} cells. Our results do suggest that during the initial seeding and outgrowth phases of metastatic peritoneal disease, localized expression of mbIL-12 can help maintain a refractory microenvironment. Understanding what triggers the switch from an active immune maintenance program toward a protumorigenic, immunosuppression program warrants further investigation.

While it is established that T effector lymphocytes can be targeted for immunomodulation by IL-12, monocytic subtypes have only recently been cited for their antitumorigenic properties in response to IL-12 immunotherapy. In a subcutaneous model of Lewis lung carcinoma (3LLC), IL-12 containing microspheres significantly reduced the expression of monocyte chemoattractant CCL2 and immunoregulatory IL-10 in TAMs within 90 min of treatment (Watkins and others 2007). CD8⁺ T cells engineered to secrete IL-12 helped establish a potent inflammatory state within the tumor microenvironment that facilitates metastatic tumor regression (Kerkar and others 2011). The latter study concluded that IL-12 acts indirectly by downregulating the accumulation of immunosuppressive myeloid-derived suppressor cells and TAMs, while improving dendritic cell antigen processing and presentation, ultimately leading to enhanced activation of CD8⁺ T effector cells within the tumor microenvironment. Thus, IL-12-mediated interactions may differ significantly depending on the resident IL-12R-bearing populations within specific microenvironments. Furthermore, the authors noted a significant IL-12-induced reduction in the Ly6C^{hi} monocytic fraction in the tumor microenvironment (Kerkar and others 2011); these cells have been proposed as the progenitor population giving rise to TAMs and TANs (Movahedi and others 2010).

It is important to reiterate that IL-12 can also have deleterious effects. In a clinical model of follicular B-cell non-

Hodgkin lymphoma, long-term IL-12 administration resulted in inferior protection and elevated serum levels of IL-12 before treatment that were associated with poor prognosis (Yang and others 2012). In fact, *in vitro* long-term IL-12 exposure was associated with an increase in TIM-3-expressing TILs and reduced IFN- γ production suggestive of IL-12-mediated immune impairment or exhaustion (Yang and others 2012). Clinical studies have also suggested adaptive responses to IL-12 therapeutic dosing, resulting in a pharmacodynamic decrease following the first dose of cytokine; this was reflected in significant decreases in IFN- γ levels and frequencies of circulating tumor-specific T cells (Bajetta and others 1998; Mortarini and others 2000).

In our study, mbIL-12 significantly delayed disease onset and the development of lethal disease. Due to the transient nature of the observed response, we surmise that the protective response elicited by mbIL-12 is dampened over time, allowing for the eventual shift toward protumorigenic signals that are more conducive for tumor outgrowth. The lack of acquired protection to rechallenge also supports the hypothesis that mbIL-12 is acting locally to maintain a balance between anti- and protumorigenic responses directly at the site of implantation. In our model, the levels of infiltrating TANs and TAMs were indicative of disease severity. Furthermore, the expression of mbIL-12 directly on the highly aggressive MOSE cell surface significantly delayed accumulation of TANs and TAMs in the OFB and PSF.

As noted, we did not find direct evidence that CD8⁺ T cells or NK cells were involved in the protective effect of mbIL-12. However, we cannot definitively rule out whether IL-12 was activating local NK cells in a manner that controlled initial outgrowth, and this will be the focus of future studies. In agreement with Kerkar and others (2011), we also observed a reduction in the number of Ly6C^{hi} monocytes present within the OFB early after MOSE-L_{F_{FLV}}/IL-12_v seeding, which may suggest a decrease in TAN and TAM progenitor populations. Alternatively, we cannot rule out the possibility that antitumor CD8⁺ responses were involved initially but were overwhelmed as tumor growth tipped the balance toward an immunosuppressive microenvironment.

Our study indicates that the poorly immunogenic MOSE-L_{F_{FLV}} cells are very efficient at establishing a protumorigenic niche within the peritoneal cavity and the OFB and that highly localized expression of mbIL-12 is transiently able to ameliorate these effects, postponing the onset of severe disease. Future kinetic studies will help determine how localized IL-12 expression is dampening the recruitment of TANs and TAMs within the tumor microenvironment as well as define the activation status of local NK cells in a time-dependent manner. While this study validates the efficacy of IL-12 as a means to mitigate peritoneal dissemination of cancer, more effective targeting strategies to deliver and sustain IL-12 within the peritoneal cavity and OFB need to be evaluated. Modifying resident immune or stromal cells within the peritoneal cavity to express mbIL-12 may offer a means to prevent metastatic or even recurrent disease and alleviate adverse side effects associated with systemic leakage of soluble IL-12 strategies.

We also envision that a targeted delivery of mbIL-12 through nanoparticles or viral vectors will allow for a similar highly localized expression in the tumor microenvironment. This could be used before surgery to assist in priming antitumor responses as well as postsurgery in a

targeted manner to stimulate removal of residual tumor cells. Interestingly, in a previous study (Cohen and others 2013b), we demonstrated that in contrast to nulliparous animals, the parous immune microenvironment in the peritoneal cavity is refractory to metastatic outgrowths. This suggests that the omental immune microenvironment can be polarized to an antimetastatic state. Highly localized IL-12 may in a similar manner to the parous microenvironment dampen recruitment of protumorigenic cells and at the same time support activation of antitumor immune responses. It remains to be determined whether the effects of mbIL-12 require an omental microenvironment or whether its effect is independent of the omentum.

In conclusion, a more comprehensive understanding of the dynamic cellular interactions during metastatic outgrowth of ovarian cancer is critical for the development of treatment strategies to effectively target the tumor microenvironment at the time of disease detection. This work provides valuable insights into the nature of the protumorigenic cascade initiated during peritoneal dissemination of cancer and highlights immune cells that could be pursued during targeted immunotherapy designed to delay or treat advanced-stage, metastatic ovarian cancer. For IL-12 immunotherapy to be effective, the cell types amenable to IL-12 targeting need to be clearly delineated and they must be mobilized to and retained within the peritoneal cavity to extend the life expectancy of ovarian cancer patients. As the OFB is often removed during surgical debulking, it will be important in future studies to determine whether the OFB or peritoneal cavity harbors the IL-12-responsive cell types important for delaying tumor outgrowth and whether they can be recruited from alternative sites in the absence of the OFB.

Acknowledgments

This work was supported, in part, by NIH R01 CA118846 (EMS, PCR) and funds provided by the Fralin Life Sciences Institute at Virginia Tech (EMS and PCR). The funding agencies had no role in the design, performance, and analyses of experiments, and writing of this report.

Author Disclosure Statement

No competing financial interests exist.

References

- Allen JW, Cardall S, Kittijarukhajorn M, Siegel CL. 2012. Incidence of ovarian maldescent in women with mullerian duct anomalies: evaluation by MRI. *AJR Am J Roentgenol* 198(4):W381–W385.
- Anderson AS, Roberts PC, Frisard MI, Hulver MW, Schmelz EM. 2014. Ovarian tumor-initiating cells display a flexible metabolism. *Exp Cell Res* 328(1):44–57.
- Ansell SM, Geyer SM, Maurer MJ, Kurtin PJ, Micallef IN, Stella P, Etzell P, Novak AJ, Erlichman C, Witzig TE. 2006. Randomized phase II study of interleukin-12 in combination with rituximab in previously treated non-Hodgkin's lymphoma patients. *Clin Cancer Res* 12(20 Pt 1): 6056–6063.
- Anwer K, Barnes MN, Fewell J, Lewis DH, Alvarez RD. 2010. Phase-I clinical trial of IL-12 plasmid/lipopolymer complexes for the treatment of recurrent ovarian cancer. *Gene Ther* 17(3):360–369.
- Atkins MB, Robertson MJ, Gordon M, Lotze MT, DeCoste M, DuBois JS, Ritz J, Sandler AB, Edington HD, Garzone PD, Mier JW, Canning CM, Battiatto L, Tahara H, Sherman ML. 1997. Phase I evaluation of intravenous recombinant human interleukin 12 in patients with advanced malignancies. *Clin Cancer Res* 3(3):409–417.
- Bajetta E, Del Vecchio M, Mortarini R, Nadeau R, Rakhit A, Rimassa L, Fowst C, Borri A, Anichini A, Parmiani G. 1998. Pilot study of subcutaneous recombinant human interleukin 12 in metastatic melanoma. *Clin Cancer Res* 4(1):75–85.
- Cohen CA, Shea AA, Heffron CL, Schmelz EM, Roberts PC. 2013a. Intra-abdominal fat depots represent distinct immunomodulatory microenvironments: a murine model. *PLoS One* 8(6):e66477.
- Cohen CA, Shea AA, Heffron CL, Schmelz EM, Roberts PC. 2013b. The parity-associated microenvironmental niche in the omental fat band is refractory to ovarian cancer metastasis. *Cancer Prev Res (Phila)* 6(11):1182–1193.
- Colombo MP, Trinchieri G. 2002. Interleukin-12 in anti-tumor immunity and immunotherapy. *Cytokine Growth Factor Rev* 13(2):155–168.
- Creekmore AL, Silkworth WT, Cimini D, Jensen RV, Roberts PC, Schmelz EM. 2011. Changes in gene expression and cellular architecture in an ovarian cancer progression model. *PLoS One* 6(3):e17676.
- Curtsinger JM, Lins DC, Mescher MF. 2003. Signal 3 determines tolerance versus full activation of naive CD8T cells: dissociating proliferation and development of effector function. *J Exp Med* 197(9):1141–1151.
- Del Vecchio M, Bajetta E, Canova S, Lotze MT, Wesa A, Parmiani G, Anichini A. 2007. Interleukin-12: biological properties and clinical application. *Clin Cancer Res* 13(16): 4677–4685.
- Gerber SA, Rybalko VY, Bigelow CE, Lugade AA, Foster TH, Frelinger JG, Lord EM. 2006. Preferential attachment of peritoneal tumor metastases to omental immune aggregates and possible role of a unique vascular microenvironment in metastatic survival and growth. *Am J Pathol* 169(5):1739–1752.
- Ghosh EE, Cassado AA, Govoni GR, Fukuhara T, Yang Y, Monack DM, Bortoluci KR, Almeida SR, Herzenberg LA, Herzenberg LA. 2010. Two physically, functionally, and developmentally distinct peritoneal macrophage subsets. *Proc Natl Acad Sci U S A* 107(6):2568–2573.
- Gray KS, Collins CM, Speck SH. 2012. Characterization of omental immune aggregates during establishment of a latent gammaherpesvirus infection. *PLoS One* 7(8):e43196.
- Humpf HU, Schmelz EM, Meredith FI, Vesper H, Vales TR, Wang E, Menaldino DS, Liotta DC, Merrill AH, Jr. 1998. Acylation of naturally occurring and synthetic 1-deoxysphinganine by ceramide synthase. Formation of N-palmitoyl-aminopentol produces a toxic metabolite of hydrolyzed fumonisin, AP1, and a new category of ceramide synthase inhibitor. *J Biol Chem* 273(30):19060–19064.
- Hunn J, Rodriguez GC. 2012. Ovarian cancer: etiology, risk factors, and epidemiology. *Clin Obstet Gynecol* 55(1): 3–23.
- Jana M, Dasgupta S, Saha RN, Liu X, Pahan K. 2003. Induction of tumor necrosis factor-alpha (TNF-alpha) by interleukin-12 p40 monomer and homodimer in microglia and macrophages. *J Neurochem* 86(2):519–528.

- Kalinski P, Hilkens CM, Wierenga EA, Kapsenberg ML. 1999. T-cell priming by type-1 and type-2 polarized dendritic cells: the concept of a third signal. *Immunol Today* 20(12):561–567.
- Kerker SP, Goldszmid RS, Muranski P, Chinnasamy D, Yu Z, Reger RN, Leonardi AJ, Morgan RA, Wang E, Marincola FM, Trinchieri G, Rosenberg SA, Restifo NP. 2011. IL-12 triggers a programmatic change in dysfunctional myeloid-derived cells within mouse tumors. *J Clin Invest* 121(12):4746–4757.
- Khan T, Heffron CL, High KP, Roberts PC. 2014. Tailored vaccines targeting the elderly using whole inactivated influenza vaccines bearing cytokine immunomodulators. *J Interferon Cytokine Res* 34(2):129–139.
- Krishnan V, Stadick N, Clark R, Bainer R, Veneris JT, Khan S, Drew A, Rinker-Schaeffer C. 2012. Using MKK4's metastasis suppressor function to identify and dissect cancer cell-microenvironment interactions during metastatic colonization. *Cancer Metastasis Rev* 31(3–4):605–613.
- Krist LF, Kerremans M, Broekhuis-Fluitsma DM, Eestermans IL, Meyer S, Beelen RH. 1998. Milky spots in the greater omentum are predominant sites of local tumour cell proliferation and accumulation in the peritoneal cavity. *Cancer Immunol Immunother* 47(4):205–212.
- Krist LF, Kerremans M, Koenen H, Blijleven N, Eestermans IL, Calame W, Meyer S, Beelen RH. 1995. Novel isolation and purification method permitting functional cytotoxicity studies of macrophages from milky spots in the greater omentum. *J Immunol Methods* 184(2):253–261.
- Lasek W, Zagozdzon R, Jakobisiak M. 2014. Interleukin 12: still a promising candidate for tumor immunotherapy? *Cancer Immunol Immunother* 63(5):419–435.
- Lenzi R, Edwards R, June C, Seiden MV, Garcia ME, Rosenblum M, Freedman RS. 2007. Phase II study of intraperitoneal recombinant interleukin-12 (rhIL-12) in patients with peritoneal carcinomatosis (residual disease < 1 cm) associated with ovarian cancer or primary peritoneal carcinoma. *J Transl Med* 5:66.
- Lenzi R, Rosenblum M, Verschraegen C, Kudelka AP, Kavanagh JJ, Hicks ME, Lang EA, Nash MA, Levy LB, Garcia ME, Platsoucas CD, Abbruzzese JL, Freedman RS. 2002. Phase I study of intraperitoneal recombinant human interleukin 12 in patients with Mullerian carcinoma, gastrointestinal primary malignancies, and mesothelioma. *Clin Cancer Res* 8(12):3686–3695.
- Leonard JP, Sherman ML, Fisher GL, Buchanan LJ, Larsen G, Atkins MB, Sosman JA, Dutcher JP, Vogelzang NJ, Ryan JL. 1997. Effects of single-dose interleukin-12 exposure on interleukin-12-associated toxicity and interferon-gamma production. *Blood* 90(7):2541–2548.
- Lim HY, Ju HY, Chung HY, Kim YS. 2010. Antitumor effects of a tumor cell vaccine expressing a membrane-bound form of the IL-12 p35 subunit. *Cancer Biol Ther* 10(4):336–343.
- Ling P, Gately MK, Gubler U, Stern AS, Lin P, Hollfelder K, Su C, Pan YC, Hakimi J. 1995. Human IL-12 p40 homodimer binds to the IL-12 receptor but does not mediate biologic activity. *J Immunol* 154(1):116–127.
- Mortarini R, Borri A, Tragni G, Bersani I, Vegetti C, Bajetta E, Pilotti S, Cerundolo V, Anichini A. 2000. Peripheral burst of tumor-specific cytotoxic T lymphocytes and infiltration of metastatic lesions by memory CD8+ T cells in melanoma patients receiving interleukin 12. *Cancer Res* 60(13):3559–3568.
- Motzer RJ, Rakhit A, Thompson JA, Nemunaitis J, Murphy BA, Ellerhorst J, Schwartz LH, Berg WJ, Bukowski RM. 2001. Randomized multicenter phase II trial of subcutaneous recombinant human interleukin-12 versus interferon-alpha 2a for patients with advanced renal cell carcinoma. *J Interferon Cytokine Res* 21(4):257–263.
- Movahedi K, Laoui D, Gysemans C, Baeten M, Stange G, Van den Bossche J, Mack M, Pipeleers D, In't Veld P, De Baetselier P, Van Ginderachter JA. 2010. Different tumor microenvironments contain functionally distinct subsets of macrophages derived from Ly6C(high) monocytes. *Cancer Res* 70(14):5728–5739.
- Nastala CL, Edington HD, McKinney TG, Tahara H, Nalesnik MA, Brunda MJ, Gately MK, Wolf SF, Schreiber RD, Storkus WJ, et al. 1994. Recombinant IL-12 administration induces tumor regression in association with IFN-gamma production. *J Immunol* 153(4):1697–1706.
- Pan WY, Lo CH, Chen CC, Wu PY, Roffler SR, Shyue SK, Tao MH. 2012. Cancer immunotherapy using a membrane-bound interleukin-12 with B7-1 transmembrane and cytoplasmic domains. *Mol Ther* 20(5):927–937.
- Rangel-Moreno J, Moyron-Quiroz JE, Carragher DM, Kusser K, Hartson L, Moquin A, Randall TD. 2009. Omental milky spots develop in the absence of lymphoid tissue-inducer cells and support B and T cell responses to peritoneal antigens. *Immunity* 30(5):731–743.
- Roberts PC, Mottillo EP, Baxa AC, Heng HH, Doyon-Reale N, Gregoire L, Lancaster WD, Rabah R, Schmelz EM. 2005. Sequential molecular and cellular events during neoplastic progression: a mouse syngeneic ovarian cancer model. *Neoplasia* 7(10):944–956.
- Rook AH, Wood GS, Yoo EK, Elenitsas R, Kao DM, Sherman ML, Witmer WK, Rockwell KA, Shane RB, Lessin SR, Vonderheid EC. 1999. Interleukin-12 therapy of cutaneous T-cell lymphoma induces lesion regression and cytotoxic T-cell responses. *Blood* 94(3):902–908.
- Schmittgen TD, Livak KJ. 2008. Analyzing real-time PCR data by the comparative C(T) method. *Nat Protoc* 3(6):1101–1108.
- Sorensen EW, Gerber SA, Sedlacek AL, Rybalko VY, Chan WM, Lord EM. 2009. Omental immune aggregates and tumor metastasis within the peritoneal cavity. *Immunol Res* 45(2–3):185–194.
- Tahara H, Zeh HJ, 3rd, Storkus WJ, Pappo I, Watkins SC, Gubler U, Wolf SF, Robbins PD, Lotze MT. 1994. Fibroblasts genetically engineered to secrete interleukin 12 can suppress tumor growth and induce antitumor immunity to a murine melanoma in vivo. *Cancer Res* 54(1):182–189.
- Tahara H, Zitvogel L, Storkus WJ, Zeh HJ, 3rd, McKinney TG, Schreiber RD, Gubler U, Robbins PD, Lotze MT. 1995. Effective eradication of established murine tumors with IL-12 gene therapy using a polycistronic retroviral vector. *J Immunol* 154(12):6466–6474.
- Trinchieri G. 2003. Interleukin-12 and the regulation of innate resistance and adaptive immunity. *Nat Rev Immunol* 3(2):133–146.
- Watkins SK, Egilmez NK, Suttles J, Stout RD. 2007. IL-12 rapidly alters the functional profile of tumor-associated and tumor-infiltrating macrophages in vitro and in vivo. *J Immunol* 178(3):1357–1362.
- Welford AF, Biziato D, Coffelt SB, Nucera S, Fisher M, Pucci F, Di Serio C, Naldini L, De Palma M, Tozer GM, Lewis CE. 2011. TIE2-expressing macrophages limit the

- therapeutic efficacy of the vascular-disrupting agent combretastatin A4 phosphate in mice. *J Clin Invest* 121(5): 1969–1973.
- Wesa A, Kalinski P, Kirkwood JM, Tatsumi T, Storkus WJ. 2007. Polarized type-1 dendritic cells (DC1) producing high levels of IL-12 family members rescue patient TH1-type antimelanoma CD4+ T cell responses in vitro. *J Immunother* 30(1):75–82.
- Yang ZZ, Grote DM, Ziesmer SC, Niki T, Hirashima M, Novak AJ, Witzig TE, Ansell SM. 2012. IL-12 upregulates TIM-3 expression and induces T cell exhaustion in patients with follicular B cell non-Hodgkin lymphoma. *J Clin Invest* 122(4):1271–1282.
- Yoo JK, Cho JH, Lee SW, Sung YC. 2002. IL-12 provides proliferation and survival signals to murine CD4+ T cells through phosphatidylinositol 3-kinase/Akt signaling pathway. *J Immunol* 169(7):3637–3643.
- Zhang L, Kerkar SP, Yu Z, Zheng Z, Yang S, Restifo NP, Rosenberg SA, Morgan RA. 2011. Improving adoptive T cell therapy by targeting and controlling IL-12 expression to the tumor environment. *Mol Ther* 19(4):751–759.

Address correspondence to:

Dr. Paul C. Roberts

*Department of Biomedical Science and Pathobiology
Virginia-Maryland College of Veterinary Medicine
Virginia Polytechnic Institute and State University
Integrated Life Sciences Building
1981 Kraft Drive (0913)
Blacksburg, VA 24061*

E-mail: pcroberts@vt.edu

Dr. Eva M. Schmelz

*Department of Human Nutrition, Foods and Exercise
Virginia Polytechnic Institute and State University
Integrated Life Sciences Building
1981 Kraft Drive (0913)
Blacksburg, VA 24061*

E-mail: eschmelz@vt.edu

Received 10 March 2015/Accepted 30 July 2015